Journal of Operation and Automation in Power Engineering

Vol. 11, No. 2, Aug. 2023, Pages: 130-143

http://joape.uma.ac.ir

A Novel Hybrid Multi-Objective Evolutionary Algorithm for Optimal Power Flow in Wind, PV, and PEV Systems

R. K. Avvari, V. Kumar D M*

Department of Electrical Engineering, National Institute of Technology Warangal,Telangana, 506004, India

Abstract-*In this paper, a new hybrid decomposition-based multi-objective evolutionary algorithm (MOEA) is proposed for the optimal power flow (OPF) problem including Wind, PV, and PEVs uncertainty with four conflicting objectives. The proposed multi-objective OPF (MOOPF) problem includes minimization of the total cost (TC), total emission (TE), active power loss (APL), and voltage magnitude deviation (VMD) as objectives and a novel constraint handling method, which adaptively adds the penalty function and eliminates the parameter dependence on penalty function evaluation is deployed to handle several constraints in the MOOPF problem. In addition, summation-based sorting and improved diversified selection methods are utilized to enhance the diversity of MOEA. Further, a fuzzy min-max method is utilized to get the best-compromised values from Pareto-optimal solutions. The impact of intermittence of Wind, PV, and PEVs integration is considered for optimal cost analysis. The uncertainty associated with Wind, PV, and PEV systems are represented using probability distribution functions (PDFs) and its uncertainty cost is calculated using the Monte-Carlo simulations (MCSs). A commonly used statistical method called the ANOVA test is used for the comparative examination of several methods. To test the proposed algorithm, standard IEEE 30, 57, and 118-bus test systems were considered with different cases and the acquired results were compared with NSGA-II and MOPSO to validate the suggested algorithm's effectiveness.*

Keyword: Wind energy, Solar energy, Multi-objective optimization, Electric vehicle, Optimal power flow.

1. INTRODUCTION

The increase in integration of renewable energy sources (RESs) and the rise in load demand is making the power system planning and operation highly challenging[1]. In power systems, the OPF is a tool for determining the optimal operating point in terms of control variables for planning and operation. The OPF aims to optimize the selective objective function by tuning the control variables and also meeting the various constraints [2, 3]. The main decision variables are the generator's real power, the magnitude of the bus voltage, the shunt compensators, and the off-nominal transformer tap settings.

In the literature, numerous scholars have proposed optimization approaches to handle the OPF problem with and without RESs. In general, two types of optimization approaches exist i) deterministic optimization techniques and ii) meta-heuristic optimization techniques. The deterministic methods are linear programming, non-linear programming, Quadratic programming, gradient technique, etc. In [4], the authors proposed a quadratic programming method to minimize power loss in the OPF problem. In [5] interior point method was proposed by the authors for solving the OPF problem. However, these deterministic approaches [6] are sensitive to initial values of the problem, sensitive to problem dimensions, and also theoretical assumptions related to problems that lead to trapping the solution to local optima. Moreover, these methods are difficult to handle mixed variable problems and constraints. It also exhibits poor convergence.

To overcome the problems with deterministic methods, various meta-heuristic methods are deployed to solve the OPF problems with and without RES. In [7], the Symbiotic organisms search (SOS) algorithm was proposed to solve security-constrained AC-DC OPF including uncertainty of Wind, PV, and PEV systems. In [8], a robust cross-entropy covariance matrix adaption evolutionary strategy (CE-CMAES) was proposed for solving the dynamic OPF problems. In this work, the dynamic OPF problem is modelled by considering the uncertainties of RESs and PEVs. In [9],

Received: 12 Mar. 2022
Revised: 31 Mar. 2022
Accepted: 02 May 2022
∗Corresponding author:
E-mail: avvari.ravi@gmail.com (Ravi Kumar Avvari)
DOI: 10.22098/JOAPE.2023.10371.1746
Research Paper

the authors proposed an SOS algorithm for resolving the optimal AC power flow problem with thermal-wind-solar-tidal systems. The uncertainties associated with wind-solar-tidal systems were modelled using Weibull, Lognormal, and Gumbel PDFs respectively. In [10], the authors developed and solved different constrained OPF problems for power systems containing RESs like wind and solar power using a hybrid modified imperialist competitive algorithm and sequential quadratic programming (HMICA-SQP). Numerous authors [11-14] focused on single-objective optimization issues in the literature. The researchers presented multi-objective optimization strategies to circumvent these limitations.

The MOEAs are gaining popularity for solving multi-objective optimization problems. The MOOPF is a non-linear, non-convex, constrained optimization problem and demands efficient methods [15]. In [16], to solve the OPF problem, a weighted sum-based differential evolutionary (DE) algorithm was presented. In this method, multiple objectives are transformed into a single-objective optimization problem by multiplying each objective with a weight such that the sum of the weights must be unity. In [17], the authors proposed a weighted sum-based Manta-Ray Foraging optimization (MRFO) algorithm to solve both single and multi-objective OPF problems with RES. The authors modified the test systems by incorporating wind and solar units at different buses and the results were analyzed for the original test system, Modification-1, and Modification-2 scenarios. In [18-20], the authors proposed weighted sum-based methods to solve the MOOPF problem. These methods are simple and easy to implement. However, the drawback of this method is, that it depends on the weights that are allocated to each objective and it fails to obtain the trade-off solutions.

In [21], the authors proposed a parallel epsilon variable multi-objective genetic algorithm (PeV-MOGA) approach for probabilistic OPF with hybrid Wind-PV-PEV systems. In this approach, the MCS was merged with the antithetic variable method (AVM) to compute the PDF of the power generated by the wind-PV-PEV system. To reduce the computational burden, the POPF problem was solved using a master-slave PeV-MOGA. In [22], a novel multi-objective glowworm swarm optimization (MO-GSO) algorithm was introduced for tackling the MOOPF in a wind integrated power system. In [23], a new hybrid algorithm based on modified GAPSO was proposed for solving the MOOPF problem. In comparison to normal PSO, PSO-GA is more trustworthy in terms of producing high-quality solutions in a fair amount of time, because the hybrid strategy avoids early convergence to local optima and allows for better exploration of the search process. In [24-26], the authors proposed Pareto dominance-based methods for the MOOPF problem. However, the Pareto-based methods suffer from limitations, such as the deterioration of selection pressure as the number of objectives increases, as a result, the effectiveness of the solution reduces.

In this work, the uncertainties associated with wind, PV, and PEV systems are represented using Weibull, lognormal and normal PDFs, and uncertainty costs are calculated using MCSs. However, in the literature, there are many uncertainties to consider and several ways to calculate the uncertainty cost. In [27], the authors introduced the stochastic optimization process by considering uncertainties in electricity demand, natural gas infrastructures, PV units, and wind generation using mixed-integer linear programming (MILP). To prove the effectiveness of the stochastic optimization approach, a modified IEEE 31-bus system was used. In [28], the authors proposed a modified Metropolis-coupled Markov chain Monte Carlo *(MC)*[3] simulation to predict the stochastic behavior of different uncertain sources. Solar radiation, wind speed, the water flow of a river, load consumption, and electricity prices are considered primary sources of uncertainty. In addition, a novel curve-fitting approach is proposed to improve the accuracy of distribution functions. Generally, MOEAs are modeled to handle conflicting goals like convergence and diversity [29].

Table1. Novelties, pros, and cons of the proposed method

<table>
<tr><th>Novelties</th><th>Pros</th><th>Cons</th></tr>
<tr><td>1. A new selection approach called summation of normalized objectives values with IDS is introduced.</td><td>1. More uniformly distributed Pareto fronts and improved convergence characteristics are obtained.</td><td>1. The performance of the algorithm depends on parameter settings.</td></tr>
<tr><td rowspan="3">2. Efficient constant handling method called the superiority of feasible solutions (SF) method is used to tackle various constants.</td><td>2. A penalty-free constraint handling technique was proposed which can handle constraints very effectively</td><td>2. Parameters are to be selected by trial and error.</td></tr>
<tr><td>3. A single run is sufficient to achieve the Pareto optimal solution.</td><td rowspan="2">3. More computational time is needed, when the number of objective functions increases.</td></tr>
<tr><td>4. It is capable of optimizing many objectives concurrently without the decision-makers knowledge</td></tr>
</table>

Convergence is about achieving a globally optimal solution, while diversity is about searching a wide search space. Since these are conflicting objectives, both cannot be optimized at a time and therefore a tradeoff between convergence and diversity is used to select a good quality solution. Hence, a novel hybrid MOEA is developed and evaluated on standard test systems for resolving the MOOPF using Wind, PV, and PEVs. In this paper, IEEE 30, 57, and 118-bus test systems were modified by adding wind, solar, and PEV energy systems. The conventional OPF itself is a large-scale, non-linear, non-convex constrained optimization problem, while integrating the Wind, PV, and PEVs, the complexity further escalates due to the intermittency of these sources. To address this problem, a new hybrid MOEA along with an effective constant handling method called superiority of feasible solutions (SF), is proposed to solve the MOOPF problem with Wind-PV-PEV.

The main contributions of the paper include:

- Proposing a unique hybrid MOEA for solving the MOOPF problem based on the decomposition and summation of normalized objectives with an enhanced diverse selection.
- Integrating Wind, PV, and PEV energy systems into the traditional OPF to investigate the effect of the stochastic nature of the sources.
- Modeling uncertainty associated with Wind, PV, and PEV systems using PDFs, and the associated uncertain cost are evaluated using Monte-Carlo simulations.
- Considering the total cost (TC), total emission (TE), APL, and VMD are the objective functions.
- Using an efficient constant handling method called the superiority of feasible solutions (SF) method to tackle various constants in the MOOPF problem.

The rest of the paper is structured as follows: Section 2 discusses the formulation of the problem. Section 3 deals with the mathematical modelling of Wind, PV, and PEV systems. Section 4 presents the proposed algorithm. Section 5 deals with simulation studies. Conclusions are made in section 6.

2. PROBLEM FORMULATION

The objectives and constants for the considered MOOPF problem are expressed as follows:

2.1. Optimization objectives

Total cost (TC):

$$\begin{aligned}\min f_{TC} = &\sum_{i=1}^{NTG}(a_i + b_i P_{TGi} + c_i P_{TGi}^2) \\ &+\sum_{j=1}^{NWG}[C_{w,j}(P_{ws,j}) + C_{Rw,j}(P_{ws,j} - P_{wav,j}) + C_{Pw,j}(P_{wav,j} - P_{ws,j})] \\ &+\sum_{k=1}^{NSG}[C_{s,k}(P_{ss,k}) + C_{Rs,k}(P_{ss,k} - P_{sav,k}) + C_{Ps,k}(P_{sav,k} - P_{ss,k})] \\ &+\sum_{l=1}^{NPEV}[C_{pev,l}(P_{pevs,l}) + C_{Rpev,l}(P_{pevs,l} - P_{pevav,l}) + C_{Ppev,l}(P_{pevav,l} - P_{pevs,l})]\end{aligned} \tag{1}$$

where f_{TC} -total cost of generation (\$/h); P_{TGi} -real power generation of a i^{th} thermal generator; a_i, b_i, c_i - i^{th} generator cost coefficients;

Total emission (TE):

$$\min f_{TE} = \sum_{i=1}^{NTG}(\alpha_i + \beta_i P_{TGi} + \gamma_i P_{TGi}^2 + \xi_i e^{\lambda_i P_{TGi}}) \tag{2}$$

where f_{TE} -total emission of generators (ton/h); $\alpha_i, \beta_i, \gamma_i, \xi_i, \lambda_i$ - i^{th} generator emission coefficients;

Active power loss (APL):

$$\min f_{APL} = \sum_{k=1}^{NL}(G_k(V_i^2 + V_j^2 - 2V_iV_j\cos\theta_{ij})) \tag{3}$$

where f_{APL} -active power loss (MW); G_k - conductance of k^{th} line;

Voltage magnitude deviation (VMD):

$$\min f_{VMD} = \sum_{i=1}^{NPQ}|(V_i - V_{ref})| \tag{4}$$

where f_{VMD} -voltage magnitude deviation (p.u.); $V_{ref} = 1.0$ p.u. i.e., reference voltage.

2.2. Constraints

Power flow constraints

$$P_{Gi} - P_{Di} - V_i\sum_{j=1}^{NB}V_j(G_{ij}\cos\theta_{ij} + B_{ij}\sin\theta_{ij}) = 0;\ i = 1,2,...NB \tag{5}$$

$$Q_{Gi} - Q_{Di} - V_i\sum_{j=1}^{NB}V_j(G_{ij}\sin\theta_{ij} - B_{ij}\cos\theta_{ij}) = 0;\ i = 1,2,...NB \tag{6}$$

Generator constraints

$$P_{TGi}^{\min} \le P_{TGi} \le P_{TGi}^{\max} \qquad i = 1,2,.............NTG \tag{7}$$

$$P_{ws,j}^{\min} \le P_{ws,j} \le P_{ws,j}^{\max} \qquad j = 1,2,..........NWG \tag{8}$$

$$P_{ss,k}^{\min} \le P_{ss,k} \le P_{ss,k}^{\max} \qquad k = 1,2,...........NSG \tag{9}$$

$$P_{pev,l}^{\min} \le P_{pev,l} \le P_{pev,l}^{\max} \qquad l = 1,2,...........NPEV \tag{10}$$

$$Q_{TGi}^{\min} \le Q_{TGi} \le Q_{TGi}^{\max} \qquad i = 1,2,.............NTG \tag{11}$$

$$Q_{ws,j}^{\min} \le Q_{ws,j} \le Q_{ws,j}^{\max} \qquad j = 1,2,.............NWG \tag{12}$$

$$Q_{ss,k}^{\min} \le Q_{ss,k} \le Q_{ss,k}^{\max} \qquad k = 1,2,..............NSG \tag{13}$$

$$V_{Gi}^{\min} \le V_{Gi} \le V_{Gi}^{\max} \qquad i = 1,2,.............NG \tag{14}$$

Shunt compensator constraints

$$Q_{Ci}^{\min} \le Q_{Ci} \le Q_{Ci}^{\max} \qquad i = 1,2,..............NC \tag{15}$$

Transformer constraints

$$T_k^{\min} \le T_k \le T_k^{\max} \qquad k = 1,2,.............NT \tag{16}$$

Security constraints

$$V_{Lp}^{\min} \le V_{Lp} \le V_{Lp}^{\max} \qquad p = 1,2,..............NLB \tag{17}$$

$$|S_{lq}| \le S_{lq}^{\max} \qquad q = 1,2,..............NL \tag{18}$$

where P_{Gi} , Q_{Gi} -real and reactive power injection at i^{th} bus; P_{Di} , Q_{Di} -real and reactive power demand at i^{th} bus ; G_{ij} , B_{ij} -conductance and susceptance between buses i and j ; NB , NTG , NWG , NSG , $NPEV$, NC , NPQ , NT , NLB and NL -number of buses, thermal generators, wind generators, solar units, PEVs, shunt VAR compensators, PQ buses, transformers, load buses and lines respectively; $P_{TGi}^{\min}$, $P_{TGi}^{\max}$ -min-max limits on i^{th} thermal generator real power; $P_{ws,j}^{\min}$, $P_{ws,j}^{\max}$ -min-max limits on j^{th} wind generator real power; $P_{ss,k}^{\min}$, $P_{ss,k}^{\max}$ -min-max limits on k^{th} solar unit real power; $P_{pev,l}^{\min}$, $P_{pev,l}^{\max}$ -min-max limits on l^{th} PEV real power; $Q_{TGi}^{\min}$, $Q_{TGi}^{\max}$ -min-max limits on i^{th} thermal generator reactive power; $Q_{ws,j}^{\min}$, $Q_{ws,j}^{\max}$ -min-max limits on j^{th} wind generator reactive power; $Q_{ss,k}^{\min}$, $Q_{ss,k}^{\max}$ -min-max limits on k^{th} solar unit reactive power; S_{lq} , $S_{lq}^{\max}$ -apparent power flow and its maximum limit respectively; $Q_{Ci}^{\min}$, $Q_{Ci}^{\max}$ -min-max limits of i^{th} shunt VAR compensator; $T_k^{\min}$, $T_k^{\max}$ -min-max limits of k^{th} transformer tap positions; $V_{Gi}^{\min}$, $V_{Gi}^{\max}$ - min-max limits of i^{th} bus voltages; θ_{ij} -voltage angle between buses i and j ;

Two equality constraints (Eqs.5 and 6) are automatically satisfied when the power flow converges to an optimal solution. The generator buses' real power (excluding slack bus), transformer tap ratios, voltage limits, and shunt compensator ranges are considered control variables that are self-limiting. The remaining inequality constraints require a constraint handling method.

3. MODELING OF STOCHASTIC WIND, PV, AND PEV SYSTEMS

In this part, the Wind, PV, and PEV systems are integrated into the conventional OPF problem. Modeling of Wind, PV, and PEV systems are discussed below:

3.1. Wind, PV, and PEV Modeling

3.1.1. Wind Energy Modelling

The wind speed distribution likely follows the Weibull PDF [30, 31]. And it is mathematically written as:

$$f(v)=\left(\frac{k}{c}\right)\left(\frac{v}{c}\right)^{(k-1)}(e)^{\left(-\frac{v}{c}\right)^k}, 0<v<\infty \tag{19}$$

where v is the wind speed (m/sec); k, c are the shape, and scale factors set at 2,10 respectively.

The power output of a wind turbine in terms of wind speed is expressed as:

$$p_w(v)=\begin{cases}0, & \text{for } v<v_{in} \text{ and } v>v_{out}\\ p_{wr}\left(\dfrac{v-v_{in}}{v_r-v_{in}}\right), & \text{for } v_{in}\le v_w\le v_r\\ p_{wr}, & \text{for } v_r<v_w\le v_{out}\end{cases} \tag{20}$$

where p_{wr} is the rated wind power output; v_{in} , v_r and v_{out} are the cut-in, rated and cut-out wind speeds with 3 m/sec, 16 m/sec, and 25 m/sec respectively.

Referring to Eq. (20), it is noticed that the power output is zero when the wind speed lies between cut-in and cut-out speeds. The wind turbine gives its rated power when the wind speed lies between its rated and cut-out speeds. The power production is continuous while the wind speed ranges between the cut-in and the rated speed. For discrete regions, the probabilities are expressed as:

$$f_w(p_w=0)=1-\exp\left(-\left(\frac{v_{in}}{c}\right)^k\right)+\exp\left(-\left(\frac{v_{out}}{c}\right)^k\right) \tag{21}$$

$$f_w(p_w=p_{wr})=\exp\left(-\left(\frac{v_r}{c}\right)^k\right)+\exp\left(-\left(\frac{v_{out}}{c}\right)^k\right) \tag{22}$$

$$f_w(p_w)=\left(\frac{k(v_r-v_{in})}{cp_{wr}}\right)\left(\frac{v_{in}p_{wr}+p_w(v_r-v_{in})}{cp_{wr}}\right)^{(k-1)}\exp\left(-\left(\frac{v_{in}p_{wr}+p_w(v_r-v_{in})}{cp_{wr}}\right)^k\right) \tag{23}$$

3.1.2. Photo-voltaic (PV) Energy Modelling

The output of a PV unit is determined by solar irradiance (G_s) which most often follows a lognormal distribution [31, 32]. The lognormal PDF is mathematically expressed as:

$$f_G(G_s)=\frac{1}{G_s\sigma\sqrt{2\pi}}\exp\left\{\frac{-(\ln G_s-\mu)^2}{2\sigma^2}\right\}, \text{for } G_s>0 \tag{24}$$

where μ and σ are the mean and standard deviations set as 6 and 0.6 respectively.

The conversion of solar irradiance to energy can be described as:

$$P_s(G_s)=\begin{cases}P_{sr}\left(\dfrac{G_s^2}{G_{std}R_c}\right) & \text{for } 0<G_s<R_c\\ P_{sr}\left(\dfrac{G_s}{G_{std}}\right) & \text{for } G_s\ge R_c\end{cases} \tag{25}$$

where G_{std} is the standard solar irradiance set to 800 W/m^2; R_c is the particular irradiance point set to 120 W/m^2; P_{sr} is the PV unit rated power output.

3.1.3. Plug-in electric vehicle (PEV) Modelling

In recent days, public transport electric vehicles ply most of the time during the day and are charged during off-peak periods and so are not suitable for V2G application. The use of privately-owned vehicles is observed to be opposite to that of public transport PEVs. The privately-owned PEVs are generally idle for most of the time during the day and hence these PEVs are suitable for the vehicle to grid (V2G) power fed capability.

The availability of electric vehicles as V2G source follows the normal distribution as follows [33]:

$$f(P_{pev}) = \frac{1}{\varphi\sqrt{2\pi}}\exp\left\{-\frac{(P_{pev}-\mu)^2}{2\varphi^2}\right\} \tag{26}$$

where μ and φ are the mean and standard deviations set as 3.2 and 0.88 respectively. P_{pev} is the available V2G power;

Here, the PEVs are used as a source of power feeding grid through suitable infrastructure. The following assumptions are made regarding the use of PEV as a power source.

- All PEVs supply battery power to the power network through DC/AC inverter.
- All PEVs represent one big V2G charging/discharging station.
- V2G system as power source controller.

Depending on the probability of PEVs available, the direct, reserve, and penalty costs are calculated

Since Wind, PV, and PEV sources are intermittent in nature, the Monte-Carlo simulations are used to account for uncertainty and to calculate the uncertainty cost. The estimated price for the intermittency of Wind, PV, and PEV powers is reflected in three ways: direct price, reserve price, and penalty price. Whenever power is underestimated, extra unusable power is wasted; however, in practical power system applications, such power can be saved in an energy storage system and thus counted as the reserve price. The price of overestimating power that is lower than the scheduled power is considered a penalty price in the case of overestimation.

3.2. Direct cost calculation of Wind, PV and PEV

Direct cost associated with j^{th} wind unit is modelled as shown below:

$$C_{w,j}(P_{ws,j}) = g_j \times P_{ws,j} \tag{27}$$

The direct cost associated with k^{th} PV unit is modelled below:

$$C_{s,k}(P_{ss,k}) = h_k \times P_{ss,k} \tag{28}$$

Similarly, the direct cost pertaining to l^{th} PEV unit is modelled below:

$$C_{pev,l}(P_{pevs,l}) = d_l \times P_{pevs,l} \tag{29}$$

where P_{ws}, P_{ss} and P_{pevs} are the scheduled powers of wind, PV, and PEV system respectively; g_j, h_k and d_l are the direct cost coefficients of j^{th} wind, k^{th} PV and l^{th} PEV systems respectively set as 1.75, 1.60, and 1.60;

3.3. Uncertainty cost calculation of wind power

When the wind farm's actual output falls short of the predicted value, the system operator must maintain a spinning reserve to ensure that consumers receive uninterrupted power. This is called overestimation of power delivered from uncertain sources and the cost incurred to maintain the spinning reserve is known as Reserve cost [30, 31]. Reserve cost associated with j^{th} wind unit is defined as:

$$C_{Rw,j}(P_{ws,j}-P_{wav,j}) = K_{Rw,j}(P_{ws,j}-P_{wav},j) = K_{Rw,j}\int_0^{P_{ws,j}}(P_{ws,j}-p_{w,j})f_w(p_{w,j})dp_{w,j} \tag{30}$$

In contrast to the overestimation case, when the actual power produced by the wind farm exceeds the predicted value, the surplus power is squandered if it cannot be utilized. As a result, the independent system operator (ISO) is required to pay a penalty fee for excess power. This is referred to as the underestimation of power delivered from uncertain sources. Penalty cost associated with j^{th} wind unit is defined as:

$$C_{Pw,j}(P_{wav,j}-P_{ws,j}) = K_{Pw,j}(P_{wav,j}-P_{ws,j}) = K_{Pw,j}\int_{P_{ws,j}}^{P_{wr,j}}(p_{w,j}-P_{ws,j})f_w(p_{w,j})dp_{w,j} \tag{31}$$

where $K_{Rw,j}$ and $K_{Pw,j}$ are the reserve and penalty cost coefficients of j^{th} wind power plant set as 3 and 1.5 respectively; $P_{wr,j}$ and $P_{wav,j}$ are the rated and actual available powers of j^{th} wind unit; $f_w(p_{w,j})$ be the possibility of j^{th} wind power.

3.4. Uncertainty cost calculation of PV

Like the wind, PV power also shows intermittency in output power. The approach to calculating the over and underestimation costs of PV is as follows [32]. Reserve cost associated with k^{th} PV plant is defined as:

$$C_{Rs,k}(P_{ss,k}-P_{sav,k}) = K_{Rs,k}(P_{ss,k}-P_{sav,k}) = K_{Rs,k} * f_s(P_{sav,k} < P_{ss,k}) * [P_{ss,k} - E(P_{sav,k} < P_{ss,k})] \tag{32}$$

Penalty cost associated with k^{th} PV plant is defined as:

$$C_{Ps,k}(P_{sav,k}-P_{ss,k})=K_{Ps,k}(P_{sav,k}-P_{ss,k})=K_{Ps,k}*f_s(P_{sav,k}>P_{ss,k})*[E(P_{sav,k}>P_{ss,k})-P_{ss,k}] \quad (33)$$

where $K_{Rs,k}$ and $K_{Ps,k}$ are the reserve and penalty cost coefficients of k^{th} PV plant respectively set as 3 and 1.5; $P_{sav,k}$ is the actual available power of k^{th} PV plant; $f_s(P_{sav,k}<P_{ss,k})$ and $f_s(P_{sav,k}>P_{ss,k})$ are the probabilities of solar power shortage and surplus respectively; $E(P_{sav,k}<P_{ss,k})$ and $E(P_{sav,k}>P_{ss,k})$ are the expectations of solar power below and above $p_{ss,k}$ respectively.

3.5. Uncertainty cost calculation of PEV

Similarly, PEVs also show intermittency in output power. The approach to calculating the over and underestimation costs of PEV is as follows [34, 35].

Reserve cost associated with l^{th} PEV is defined as:

$$C_{Rpev,l}(P_{pevs,l}-P_{pevav,l})=K_{Rpev,l}(P_{pevs,l}-P_{pevav,l})=K_{Rpev,l}\int_0^{P_{pev,l}}(P_{pevs,l}-p_{pev,l})f_{pev}(p_{pev,l})dp_{pev,l} \quad (34)$$

Penalty cost associated with l^{th} PEV is defined as:

$$C_{Ppev,l}(P_{pevav,l}-P_{pevs,l})=K_{Ppev,l}(P_{pevav,l}-P_{pevs,l})=K_{Ppev,l}\int_{P_{pevs,l}}^{P_{pevr,l}}(p_{pev,l}-P_{pevs,l})f_{pev}(p_{pev,l})dp_{pev,l} \quad (35)$$

where $K_{Rpev,l}$ and $K_{Ppev,l}$ are the reserve and penalty cost coefficients of l^{th} PEV set as 3 and 1.5 respectively; $P_{pevr,l}$ and $P_{pev,l}$ are the rated and actual available powers of l^{th} PEV respectively; $f_{pev}(p_{pev,l})$ is the l^{th} PEV power probability.

3.6. Constraint Handling Method (CHM)

A CHM must be used in conjunction with an evolutionary algorithm to guide the search process toward a globally optimal solution. Among the many CHMs, the most frequently employed is the penalty approach, which involves adding a penalty to the fitness of a non-feasible solution. Despite its simplicity and ease of implementation, this method's performance is highly dependent on the penalty factor, which must be calibrated through trial and error. To tackle this difficulty, in this study a new parameter-free CHM superiority of feasible solution (SF) is introduced in the study for solving the MOOPF problem.

In [36], Deb introduced the SF method for handling different constraints efficiently. In the SF method, a comparison is drawn between a pair of solutions. When a pair of solutions is compared, the following cases emerge:

(1) While comparing two non-feasible solutions, the solution having the smallest constraint violation is selected.

(2) When two feasible solutions are compared, the one with a better fitness solution is selected.

(3) When a feasible solution is compared to a non-feasible solution, the feasible solution is selected.

Comparing non-feasible solutions based on constraint violation helps push non-feasible answers into the feasible region while comparing viable solutions based on the fitness value enables solution quality to be improved.

By incorporating these three rules into the proposed algorithm to solve the MOOPF problem, two situations arise, the first of which is when the population size is lower than the number of feasible solutions, and the second method is to ignore non-feasible solutions. The use of the summation-based method is to select feasible solutions if the number of feasible solutions is greater than the population size.

4. PROPOSED ALGORITHM

The MOEAs are normally modeled to handle different conflicting goals, such as maximizing the spread of solutions along the Pareto front (i.e., diversity) and minimizing the distance between the solutions along the Pareto front (i.e., convergence) [37]. The trade-off between convergence and diversity is important to choose the best solution among the obtained solutions. Therefore, a new strategy is proposed in this study to strike a compromise between convergence and diversity.

In this paper, a summation of normalized objective values (SNOV) with improved diversified selection (IDS) is suggested and integrated with the multi-objective evolution algorithm based on the decomposition (MOEA/D) [38] method to solve the MOOPF problem with RES. The MOEA/D method decomposes the multi-objective optimization problem into several single scalar optimization problems and optimizes them all at the same time using weight vectors. The weight vectors' distance is used to create neighborhoods. In every population evolution, information from the neighborhood is used to find a solution. The non-dominated sorting used in MOEA/D is complex and time-taking. Some useful information may be lost if the dominant solutions are completely discarded. In addition, diversity may be lost during the search process and lead to local optima. To overcome these problems, the summation of normalized objectives values [39] with IDS is employed in this paper instead of non-dominated sorting selection to get uniformly distributed Pareto front and improved convergence characteristics.

A new constraint handling strategy called the superiority of feasible solutions (SF) approach is employed to tackle various constraints (i.e. equality and inequality) of the MOOPF problem. The suggested algorithm employs the fuzzy method to get the best-compromised values. The outcomes of the suggested method are compared with popular methods like NSGA-II [40] and MOPSO [41] for different cases.

The main steps in the proposed method can be stated as follows:

Step 1: Input:

- Dimensions of the problem.
- Population size (*N*).
- Stopping criteria.
- Decision variable size.
- Limits of decision variables in vector form.
- Control parameters of the corresponding method.
- Test system data.

Step 2: Initialization:

- POP: Generate an initial population (Pt) of size *N*.
- Generate uniformly distributed weight vectors using a systematic sampling approach (SSA) [42] with the number of weight vectors defined as:

$$N(D,M)=\binom{D+M-1}{M-1} \tag{36}$$

where M be the number of objective functions.

- Run the load flow, and calculate the fitness of the selected objective and total constraint violation.
- Locate neighbors with the smallest angles for each weight vector using angle criteria [43] as follows:

$$\tan\theta=\frac{d_2}{d_1} \tag{37}$$

$$d_1=\frac{\left\|w_i^T w_j\right\|}{\left\|w_j\right\|},\ d_2=\left\|w_i-d_1\frac{w_j}{\left\|w_j\right\|}\right\| \tag{38}$$

where w_i, w_j are the weight vectors.

- Find the smallest objective values to form the present ideal point.
- Find the largest objective values to form the present nadir point.
- Set iteration count=1.

Step 3: Reproduction:

- Use an angle criterion to choose *N* pair of mating parents. A set of mating parents is picked from neighbors with a probability of δ for each weight vector.
- Perform two-point crossover and mutation operations to generate a new population (Qt).
- Calculate the fitness of objective functions for the newly generated population (Qt).
- Calculate the total constraint violation for the new population (Qt).
- Merge the original population (Pt) and the new population (Qt).

Step 4: Investigation of feasible solutions:

- Sort the total population ascending by total constraint violation values.
- Discover feasible solutions.
- If the number of feasible solutions is lower than the population size (*N*), **Go to Step 6.**
- If minimum *N* feasible solutions exist in the combined population, **Go to Step 5.**

Step 5: Normalization and selection:

- Determine the normalized objective value for each objective and solution using the below equation [39, 44].

$$f_i^{''}(x^m)=\frac{f_i(x^m)-f_{i,\min}}{f_{i,\max}-f_{i,\min}} \tag{39}$$

where $f_i^{''}(x^m)$ is the normalized value of x^m for i -th objective, $f_{i,\min}$, $f_{i,\max}$ are the min, max.values of the i -th objective.

- Obtain a summation of the normalized objective values for all solutions [39, 44].

$$F^{''}(x^m)=\sum_{i=1}^{M} f_i^{''}(x^m) \tag{40}$$

- Calculate the Euclidian distance between the origin and the sum of all normalized objective values. The stopping point is determined by the solution that produces total normalized objective values close to the origin.
- Equally, divide the objective space into 100 bins where scanning of the bins should continue until the scanning procedure reaches a stopping point. The solution with the shortest sum of normalized objective values is chosen to enter the preferred set for each scanned bin.
- The backup set includes unselected solutions as well as solutions dominated by the stopping point.

Step 6: Termination:

- Increase iteration number by one i.e. iter=iter+1.

- If the stopping requirement is met, Stop else Go to Step 3.

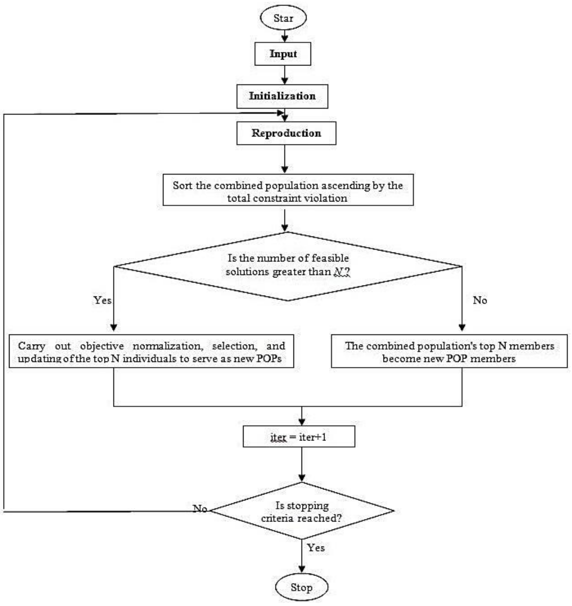

Fig.1. Flow chart of the suggested method

5. SIMULATION AND RESULTS

To evaluate the efficacy of the suggested method, it is implemented on three test systems, namely, IEEE 30, 57, and 118-bus power systems. The suggested method for the MOOPF problem was executed in MATLAB R2016a and the simulations were carried out on i3-Processor with 4GB RAM.

Table 2. Control parameters of various methods

S. No.	Method	Control Parameters
1.	Proposed Method	Population size (N) =100, No. of divisions made along with every object (D) =12, neighbourhood size (T) =20, Crossover rate (P_c) =1.0, Mutation rate (P_m) =0.05, No. of iterations=100.
2.	NSGA-II [40]	Population size (N) =100, No. of iterations=100, Crossover rate (P_c) =0.8, Mutation rate (P_m) =0.01.
3.	MOPSO [41]	Population size (N) =100, C1=C2=2, W=0.5, No. of iterations=100.

Table 3. Various cases considered in this paper

S. No	Test system	Case	TC	TE	APL	VMD
1.	IEEE 30-bus system	Case-1	✓	✓	-	-
		Case-2	✓	-	✓	-
		Case-3	✓	✓	✓	-
		Case-4	✓	✓	-	✓
		Case-5	✓	✓	✓	✓
2.	IEEE 57-bus system	Case-6	✓	✓	-	-
		Case-7	✓	-	✓	-
		Case-8	✓	✓	✓	-
		Case-9	✓	✓	-	✓
		Case-10	✓	✓	✓	✓
3.	IEEE 118-bus system	Case-11	✓	-	✓	-
		Case-12	✓	-	✓	✓

5.1. Modified IEEE 30-bus system

The IEEE 30-bus power system has 6 thermal generators placed at buses 1, 2, 5,8,11, and 13 (# 1 generator acts as a slack generator) with 41 lines. In this paper, 4 off-nominal transformers are considered between lines 6-10, 6-9, 4-12, and 27-28 and 9 shunt VAR compensators are placed at the buses. The whole real and reactive power demand on the system is 238.40MW and 126.20MVAR respectively [45]. In addition to the above, the system is modified by connecting Wind, PV, and PEV systems at buses 21, 7, and 30 respectively.

5.1.1. Case-1: Minimize TC and TE simultaneously

In this case, TC and TE are the objectives considered for minimizing simultaneously. The optimal decision variables obtained by the suggested method are included in Table 4. The best-compromised values using the proposed algorithm have a TC of 858.9256$/h and TE of 0.2093ton/h which is the lowest value compared with NSGA-II [40] and MOPSO [41] as reported in Table 5. The best-compromised values achieved using the above methods are 859.9519$/h, 0.2101ton/h, and 863.2138$/h, 0.2116ton/h respectively. Fig. 2 depicts the Pareto optimal (PO) fronts for each approach.

5.1.2. Case-2: Minimize TC and APL simultaneously

In this case, TC and APL are the objectives that need to be minimized simultaneously. The optimal decision variables obtained by the suggested method are included in Table 4. The best-compromised values using the proposed algorithm have a total cost of 853.6756$/h and an APL of 2.3263MW which is the lowest value compared with NSGA-II [40] and MOPSO [41] as reported in Table 5. The best-compromised values achieved using the above methods are 855.2758$/h, 2.4230MW, and 858.9110$/h, 2.5328MW respectively. Fig. 3 depicts the PO fronts for each approach.

5.1.3. Case-3: Minimize TC, TE and APL simultaneously

In this case, TC, TE, and APL are the objectives that need to be minimized simultaneously. The optimal decision variables obtained by the suggested method are included in Table 4. The best-compromised values using the proposed algorithm have a TC of 868.3559$/h, TE of 0.2079ton/h, and APL of 2.1775MW which is the lowest value compared with NSGA-II [40] and MOPSO [41] as reported in Table 5. The best compromised values achieved using the above methods are 869.2563$/h, 0.2078ton/h, 2.3740MW and 876.5231$/h, 0.2058ton/h, 3.2157MW respectively. Fig.4 depicts the PO fronts for each approach.

5.1.4. Case-4: Minimize TC, TE and VMD simultaneously.

In this case, TC, TE, and VMD are the objectives considered for minimizing simultaneously. The optimal decision variables obtained by the suggested method are included in Table 4. The best-compromised values using the proposed algorithm have a TC of 842.3661$/h, TE of 0.2184ton/h, and VMD of 0.0973p.u.which is the lowest value compared with NSGA-II [40] and MOPSO [41] as reported in Table 5. The best compromised values achieved using the above methods are 843.7067$/h, 0.2154ton/h, 0.1335p.u.and 854.4809$/h, 0.2142ton/h, 0.1606p.u.respectively. Fig. 5 depicts the PO fronts for each approach.

5.1.5. Case-5: Minimize TC, TE, APL, and VMD simultaneously.

In this case, TC, TE, APL, and VMD are the objectives considered to be minimized simultaneously. The optimal decision variables obtained by the suggested method are included in Table 4. The best-compromised values using the proposed algorithm have a TC of 865.0922$/h, TE of 0.2095ton/h, APL of 2.2978MW, and VMD of 0.1336p.u. which is the lowest value compared with NSGA-II [40] and MOPSO [41] as reported in Table 5. The best compromised values achieved using the above methods are 869.8337$/h, 0.2107ton/h, 2.5380MW, 0.2561p.u.and 918.3540$/h, 0.2026ton/h, 1.8499MW, 0.1804p.u. respectively.

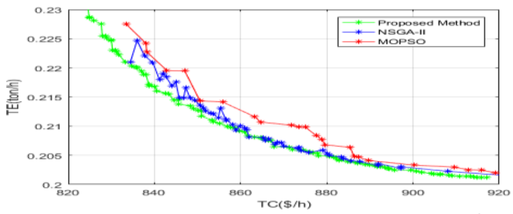

Fig.2.Case-1: IEEE 30-bus system Pareto optimal fronts

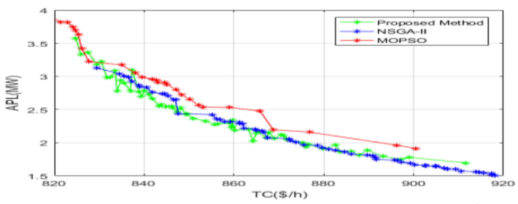

Fig.3. Case-2: IEEE 30-bus system Pareto optimal fronts

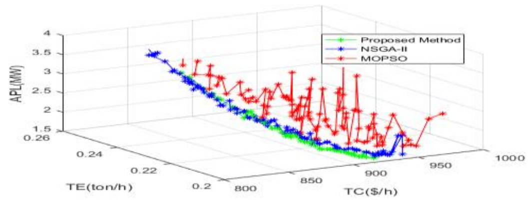

Fig.4. Case-3: IEEE 30-bus system Pareto optimal fronts

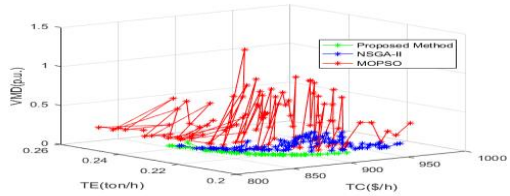

Fig.5. Case-4: IEEE 30-bus system Pareto optimal fronts

Table 4. IEEE 30-bus system: best-compromised values achieved by the suggested method for Case-1 to 5

S.No.	Control variables	Control variables at bus/line	Limits Min	Limits Max	Case-1	Case-2	Case-3	Case-4	Case-5
1.	Power (MW)	2	20	80	45.9458	43.7045	45.7895	45.0363	45.0262
2.		5	15	50	27.8704	32.3782	32.0212	24.5831	31.3830
3.		8	10	35	25.4106	22.3175	22.3489	20.9377	25.9356
4.		11	10	30	23.7889	15.9720	22.8090	16.0211	18.7876
5.		13	12	40	26.8761	18.4583	23.7380	22.8131	23.3002
6.		21	0	50	34.2826	38.0159	36.5405	33.2034	34.9378
7.		7	0	50	36.6994	44.6478	41.7745	41.6915	41.3679
8.		30	0	15	3.4689	8.9195	8.1977	9.6364	9.8781
9.	Voltage (p.u)	1	0.95	1.1	1.0366	1.0412	1.0395	1.0115	1.0296
10.		2	0.95	1.1	1.0239	1.0339	1.0323	1.0098	1.0199
11.		5	0.95	1.1	0.9942	1.0128	1.0103	0.9947	0.9953
12.		8	0.95	1.1	1.0172	1.0213	1.0238	0.9926	1.0028
13.		11	0.95	1.1	1.0222	1.0305	1.0377	1.0176	0.9882
14.		13	0.95	1.1	1.0210	1.0386	1.0291	1.0192	1.0209
15.	Tap ratio	11	0.9	1.1	0.9851	0.9929	1.0002	1.0266	1.0108
16.		12	0.9	1.1	0.9905	0.9912	1.0128	1.0231	1.0012
17.		15	0.9	1.1	1.0200	0.9904	0.9873	0.9744	0.9872
18.		36	0.9	1.1	0.9873	0.9814	0.9976	0.9859	0.9827
19.	Shunt VAR compensator (MVAR)	10	0	5	2.0773	2.2870	2.8454	2.2417	2.2433
20.		12	0.	5	2.8681	2.2815	5.5854	2.4882	3.5771
21.		15	0	5	2.2181	3.0105	3.8380	2.2779	2.2404
22.		17	0	5	1.5441	2.4913	2.5731	1.9535	2.3970
23.		20	0	5	2.1519	2.7815	2.8305	4.0611	3.2049
24.		21	0	5	2.1637	2.3464	2.2532	1.7295	2.5201
25.		23	0	5	2.0966	2.4114	1.4699	3.1976	2.6193
26.		24	0	5	2.8898	2.8234	3.0354	3.6187	2.9410
27.		29	0	5	2.6363	2.4902	3.1590	3.4609	1.8377
1.	TC($/h)	-	-	-	858.9256	853.6756	868.3559	842.3661	865.0922
2	TE(ton/h)	-	-	-	0.2093	-	0.2079	0.2184	0.2095
3.	APL(MW)	-	-	-	-	2.3263	2.1775	-	2.2978
4.	VMD(p.u.)	-	-	-	-	-	-	0.0973	0.1336

Table 5. IEEE 30-bus system: Comparison of the suggested method with NSGA-II [40] and MOPSO [41] for Case-1 to 5

Case Name	Objective Functions	Proposed Method	NSGA-II [40]	MOPSO [41]
Case-1	TC($/h)	858.9256	859.9519	863.2138
	TE(ton/h)	0.2093	0.2101	0.2116
Case-2	TC($/h)	853.6756	855.2758	858.9110
	APL(MW)	2.3263	2.4230	2.5328
Case-3	TC($/h)	868.3559	869.2563	876.5231
	TE(ton/h)	0.2079	0.2078	0.2058
	APL(MW)	2.1775	2.3740	3.2157
Case-4	TC($/h)	842.3661	843.7067	854.4809
	TE(ton/h)	0.2184	0.2154	0.2142
	VMD(p.u.)	0.0973	0.1335	0.1606
Case-5	TC($/h)	865.0922	869.8337	918.3540
	TE(ton/h)	0.2095	0.2107	0.2026
	APL(MW)	2.2978	2.5380	1.8499
	VMD(p.u.)	0.1336	0.2561	0.1804

5.2. Modified IEEE 57-bus system

To demonstrate the scalability of the proposed approach, the MOOPF problem is solved using the IEEE 57-bus system. It contains 7 thermal generators placed at buses 1, 2, 3, 6, 8, 9, and 12 (# 1 generator acts as a slack generator) with 80 lines. In this paper, 15 off-nominal transformers are considered along with 3 shunt VAR compensators. The entire real and reactive power demand on the system is 1250.80MW and 336.40MVAR respectively [45]. The standard system is modified by connecting Wind, PV, and PEV systems at buses 45, 16, and 49 respectively.

5.2.1. Case-6: Minimize TC and TE simultaneously

In this case, TC and TE are the objectives that need to be minimized simultaneously. The optimal decision variables obtained by the recommended method are included in Table 6. The best compromise solution using the proposed algorithm has a TC of 35815.04$/h and TE of 0.8950ton/h which is the lowest value compared with NSGA-II [40] and MOPSO [41] as reported in Table 7. The best-compromised values achieved using the above methods are 35850.00$/h, 0.9928ton/h, and 35910.00$/h, 1.0120ton/h respectively. Fig. 6 depicts the PO fronts for each approach.

5.2.2. Case-7: Minimize TC and APL simultaneously

In this case, TC and APL are the objectives that need to be minimized simultaneously. The optimal decision variables obtained by the suggested method are included in Table 6. The best compromise solution using the proposed algorithm has a total cost of 35169.27$/h and an APL of 9.8050MW which is the lowest value compared with NSGA-II [40] and MOPSO [41] as reported in Table 7. The best-compromised values achieved using the above methods are 35344.00$/h, 9.9855MW, and 35404.00$/h, 11.2682MW respectively. Fig. 7 depicts the PO fronts for each approach.

5.2.3. Case-8: Minimize TC, TE and APL simultaneously

In this case, TC, TE, and APL are the objectives that need minimizing simultaneously. The optimal decision variables obtained by the suggested method are included in Table 6. The best-compromised values using the proposed algorithm have a TC of 35558.26$/h, TE of 0.9673ton/h, and APL of 10.0796MW, which is the lowest value compared with NSGA-II [40] and MOPSO [41] as reported in Table 7. The best compromised values achieved using the above methods are 36336.00$/h, 1.2498ton/h, 11.0813MW and 36402.69$/h, 1.0450ton/h, 12.5591MW respectively. Fig. 8 depicts the PO fronts for each approach.

5.2.4. Case-9: Minimize TC, TE and VMD simultaneously

In this case, TC, TE, and VMD are the objectives that need minimizing simultaneously. The optimal decision variables obtained by the suggested method are included in Table 5. The best-compromised values using the proposed algorithm have a TC of 35888.04$/h, TE of 0.9012ton/h, and VMD of 0.7043p.u. which is the lowest value compared with NSGA-I[40] and MOPSO [41] as reported in Table 6. The best compromised values achieved using the above methods are 36224.00$/h, 0.9074 ton/h, 0.8284p.u. and 36989.00$/h, 1.0916ton/h, 0.8060p.u. respectively. Fig.9 depicts the PO fronts for each approach.

5.2.5. Case-10: Minimize TC, TE, APL, and VMD simultaneously

In this case, TC, TE, APL, and VMD are the objectives that need to be minimized simultaneously. The optimal decision variables obtained by the suggested method are included in Table 6. The best-compromised values using the proposed algorithm have a TC of 35980.02$/h, TE of 1.1696ton/h, APL of 10.5229MW, and VMD of 0.8308p.u. which is the lowest value compared with NSGA-II [40] and MOPSO [41] as reported in Table 7. The best compromised values achieved using above methods are 36250.00$/h, 1.4175ton/h, 12.3871MW, 1.0481p.u. and 36662.59$/h, 0.9367ton/h, 14.1833MW, 1.0669p.u respectively.

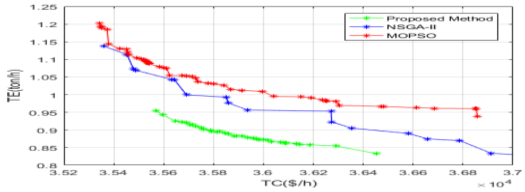

Fig.6. Case-6: IEEE 57-bus system Pareto optimal fronts

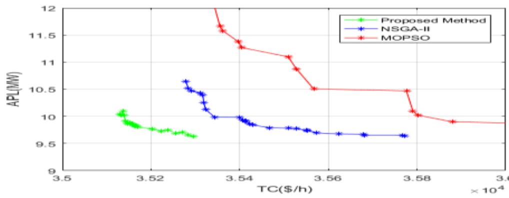

Fig.7. Case-7: IEEE 57-bus system Pareto optimal fronts

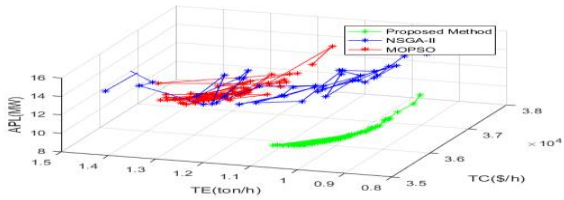

Fig.8. Case-8: IEEE 57-bus system Pareto optimal fronts

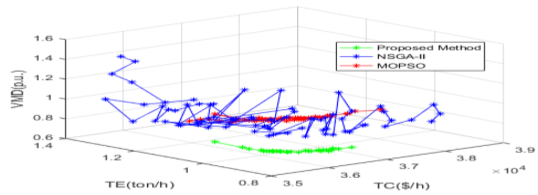

Fig.9. Case-9: IEEE 57-bus system Pareto optimal fronts

5.3. Modified IEEE 118-bus system

To show the scalability of the proposed algorithm for a large-scale test system in solving the MOOPF problem, IEEE 118-bus system was considered. It contains 54 thermal generators (# 69 generator as a slack generator), and 186 lines. In this paper, 9 off-nominal transformers and 12 shunt VAR compensators are considered. The sum of real and reactive power demand on the system is 4242.00MW and 1439.00MVAR respectively [45]. The test system is modified by connecting Wind, PV, and PEV systems at buses 81, 64, and 117 respectively.

5.3.1. Case-11: Minimize TC and APL simultaneously

In this case, TC and APL are the objectives that need to be minimized simultaneously. The optimal decision variables obtained by the suggested method are included in Table 8. The best compromise values using the suggested algorithm have a total cost of 129019.12$/h and APL of 36.7616MW, which is the lowest value compared with NSGA-II [40] and MOPSO [41] as reported in Table 8. The best-compromised values achieved using the above methods are 129582.23$/h, 37.3464MW, and 130673.5$/h, 38.0368MW respectively. Fig. 10 depicts the PO fronts for each approach.

Table 6. IEEE 57-bus system: best-compromised values achieved by the proposed method for Case-6 to 10

S.No.	Control variables	Control variables at bus/line	Limits Min	Limits Max	Case-6	Case-7	Case-8	Case-9	Case-10
1.	Power (MW)	2	0	100	95.7907	25.0904	84.1793	100.0000	57.9085
2.		3	0	140	69.0738	49.7571	53.1935	75.5083	80.1009
3.		6	0	100	97.6214	54.1223	95.7712	79.7732	57.4498
4.		8	0	550	304.0230	369.2352	302.8312	314.7732	329.5786
5.		9	0	100	82.3521	70.0209	98.7022	83.9870	64.9448
6.		12	0	410	294.0245	384.9806	331.1684	282.9023	379.1110
7.		45	0	80	79.8467	79.8727	79.7886	79.4149	78.2859
8.		16	0	80	79.7469	79.9213	79.9465	79.8968	78.5326
9.		49	0	20	19.3799	19.9008	19.8993	19.6642	14.6734
10.	Voltage (p.u)	1	0.95	1.1	1.0385	1.0398	1.0340	1.0394	1.0226
11.		2	0.95	1.1	1.0279	1.0305	1.0286	1.0267	1.0102
12.		3	0.95	1.1	1.0313	1.0244	1.0252	1.0227	1.0144
13.		6	0.95	1.1	1.0343	1.0185	1.0203	1.0228	1.0127
14.		8	0.95	1.1	1.0394	1.0135	1.0201	1.0253	1.0224
15.		9	0.95	1.1	1.0214	1.0013	1.0123	1.0102	1.0125
16.		12	0.95	1.1	1.0341	1.0209	1.0353	1.0217	1.0421
17.	Tap ratio	19	0.9	1.1	1.0362	1.0148	1.0016	1.0159	1.0101
18.		20	0.9	1.1	1.0250	0.9987	0.9939	1.0109	0.9964
19.		31	0.9	1.1	1.0036	0.9842	0.9826	0.9953	1.0142
20.		35	0.9	1.1	1.0307	0.9945	1.0275	0.9830	0.9855
21.		36	0.9	1.1	0.9769	0.9873	0.9881	1.0323	0.9927
22.		37	0.9	1.1	1.0448	1.0182	1.0359	0.9926	1.0270
23.		41	0.9	1.1	1.0065	1.0187	0.9990	1.0269	1.0064
24.		46	0.9	1.1	0.9927	0.9800	0.9800	0.9426	0.9956
25.		54	0.9	1.1	1.0014	0.9573	0.9536	0.9030	0.9065
26.		58	0.9	1.1	0.9821	0.9654	0.9724	0.9762	0.9780
27.		59	0.9	1.1	0.9530	0.9667	0.9719	0.9575	0.9732
28.		65	0.9	1.1	0.9719	0.9724	0.9847	0.9902	0.9799
29.		66	0.9	1.1	0.9873	0.9397	0.9485	0.9260	0.9536
30.		71	0.9	1.1	0.9720	0.9465	0.9750	0.9538	0.9620
31.		73	0.9	1.1	0.9815	0.9910	1.0087	1.0263	1.0091
32.		76	0.9	1.1	0.9844	0.9750	0.9706	0.9188	0.9641
33.		80	0.9	1.1	1.0118	0.9906	0.9973	1.0165	1.0106
34.	Shunt VAR compensator (MVAR)	18	0	20	11.6868	10.7152	8.9393	7.2739	11.0809
35.		25	0	20	10.5195	11.2397	10.2799	13.0381	11.1002
36.		53	0	20	10.8182	8.9104	6.1637	10.1057	8.4158
1.	TC($/h)	-	-	-	35815.04	35169.27	35558.26	35888.04	35980.02
2.	TE(ton/h)	-	-	-	0.8950	-	0.9673	0.9012	1.1696
3.	APL(MW)	-	-	-	-	9.8050	10.0796	-	10.5229
4.	VMD(p.u.)	-	-	-	-	-	-	0.7043	0.8308

Table 7. IEEE 57-bus system: Comparison of the suggested method with NSGA-II [40] and MOPSO [41] for Case-6 to 10

Case Name	Objective Functions	Proposed Method	NSGA-II [40]	MOPSO [41]
Case-6	TC($/h)	35815.04	35850.00	35910.00
	TE(ton/h)	0.8950	0.9928	1.0120
Case-7	TC($/h)	35169.27	35344.00	35404.00
	APL(MW)	9.8050	9.9855	11.2682
Case-8	TC($/h)	35558.26	36336.00	36402.69
	TE(ton/h)	0.9673	1.2498	1.0450
	APL(MW)	10.0796	11.0813	12.5591
Case-9	TC($/h)	35888.04	36224.00	36989.00
	TE(ton/h)	0.9012	0.9074	1.0916
	VMD(p.u.)	0.7043	0.8284	0.8060
Case-10	TC($/h)	35980.02	36250.00	36662.59
	TE(ton/h)	1.1696	1.4175	0.9367
	APL(MW)	10.5229	12.3871	14.1833
	VMD(p.u.)	0.8308	1.0481	1.0669

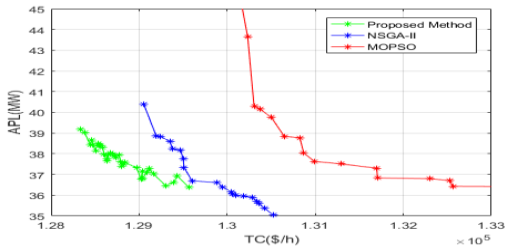

Fig.10. Case-11: IEEE 118-bus system Pareto optimal fronts

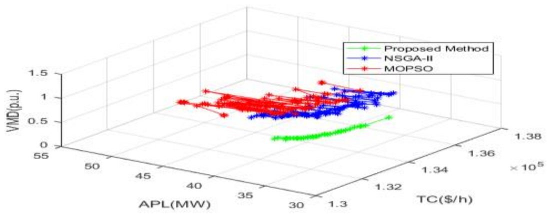

Fig.11. Case-12: IEEE 118-bus system Pareto optimal fronts

Table 8. IEEE 118-bus system: best-compromised values for Case-11 and Case-12

S. No.	Control variables	Bus / line	Limits Min	Limits Max	Case-11 Proposed Method	Case-11 NSGA-II [40]	Case-11 MOPSO [41]	Case-12 Proposed Method	Case-12 NSGA-II [40]	Case-12 MOPSO [41]
1.	Power (MW)	1	0	100	40.0447	48.3405	63.6501	63.4515	33.3504	63.3967
2.		4	0	100	49.9982	48.9338	53.5327	35.6629	33.2645	49.8530
3.		6	0	100	59.1167	59.3328	47.0428	35.0138	42.7372	55.9243
4.		8	0	100	45.0837	44.6111	33.9415	47.8259	37.5502	42.1967
5.		10	0	550	193.3528	198.6711	225.9731	164.2240	212.8393	188.3711
6.		12	0	185	66.1489	65.9076	77.3970	76.0734	88.2417	86.2172
7.		15	0	100	48.9935	49.1643	56.4980	56.2799	43.1842	47.2287
8.		18	0	100	43.7256	43.0544	38.1805	39.0496	58.9581	51.8238
9.		19	0	100	28.7879	28.7425	56.6487	70.2897	41.3202	60.0969
10.		24	0	100	33.8075	37.6122	41.0475	48.7321	55.7882	41.0988
11.		25	0	320	120.0409	119.1804	91.3385	60.8414	105.1466	106.7849
12.		26	0	414	120.6440	125.8632	139.7833	169.9155	133.5220	138.8390
13.		27	0	100	46.2456	46.4613	42.2751	61.7409	59.3025	41.7592
14.		31	0	107	22.3999	23.2030	14.1244	22.4692	15.4927	26.9107
15.		32	0	100	55.1251	55.1034	43.5945	27.1559	29.6347	53.5314
16.		34	0	100	51.6765	49.7872	30.0776	56.3221	50.3974	43.8198
17.		36	0	100	55.7278	55.8064	46.3354	26.4301	47.3615	38.8550
18.		40	0	100	58.4597	53.2461	59.4651	54.2550	45.0434	49.0854
19.		42	0	100	61.1690	55.9346	49.2207	78.9208	58.3905	43.4171
20.		46	0	119	42.4237	41.7433	32.4406	36.1427	54.2950	48.1913
21.		49	0	304	178.0395	148.7433	183.1493	177.0897	131.1200	184.0774
22.		54	0	148	68.7727	61.9638	69.9576	93.0152	84.6901	54.0201
23.		55	0	100	41.4856	40.9559	43.8303	64.4180	44.6150	60.1522
24.		56	0	100	56.0731	52.8332	56.7499	39.1371	53.4836	51.1180
25.		59	0	255	141.0298	123.3472	152.7499	133.8940	165.7378	117.9661
26.		61	0	260	106.4001	105.3442	125.3087	112.9721	60.7726	106.7391
27.		62	0	100	60.9986	61.0078	33.7938	56.6838	57.5269	49.1312
28.		65	0	491	220.8742	220.5479	226.5447	232.4857	200.8274	228.0551
29.		66	0	492	204.3118	208.6433	171.8156	137.5718	207.0259	192.0830
30.		70	0	100	57.4597	59.8371	20.1797	45.9800	59.0853	58.5005
31.		72	0	100	40.2247	39.6023	45.6147	35.5260	32.2217	52.1747
32.		73	0	100	33.4507	33.2678	44.7217	40.8232	50.1046	43.8125
33.		74	0	100	62.6285	49.9213	63.6268	52.5801	54.5198	44.4446
34.		76	0	100	58.4179	58.0876	49.2420	60.1585	56.9626	46.9866
35.		77	0	100	58.7759	59.6641	45.42557	47.9148	68.9018	54.1347
36.		80	0	577	277.4328	275.5281	251.2416	307.3935	213.9730	262.9793
37.		85	0	100	45.6938	45.1100	25.9303	50.9420	41.9730	44.7471
38.		87	0	104	8.7870	8.4396	5.1801	9.0718	22.7264	15.9175
39.		89	0	707	265.9201	266.5600	323.5939	217.2268	253.6893	234.4638
40.		90	0	100	37.1972	37.4954	48.6774	40.2967	42.9491	47.3719
41.		91	0	100	38.8539	38.8713	44.3201	31.8664	40.5407	43.0382
42.		92	0	100	48.4612	53.1343	25.9523	49.3316	51.6978	44.1538
43.		99	0	100	37.8606	38.6321	13.4615	30.9745	50.4100	54.8767
44.		100	0	352	97.0986	96.8499	125.8402	130.9657	138.1789	123.3379
45.		103	0	140	71.3612	71.9647	55.1600	50.4524	63.5971	50.3507
46.		104	0	100	54.0455	53.9685	47.1531	51.1611	43.8495	52.8388
47.		105	0	100	37.9765	36.6977	31.9361	43.3539	31.4387	47.6009
48.		107	0	100	46.0688	47.0195	37.6778	38.7497	40.0955	37.4718
49.		110	0	100	41.2868	40.7633	27.3572	31.8345	37.3201	36.9108
50.		111	0	136	30.3153	40.2204	42.3744	42.3214	52.6251	53.6456
51.		112	0	100	38.6270	38.9172	37.9132	34.9093	43.7788	33.6974
52.		113	0	100	51.6430	51.4637	36.8854	44.9313	61.3156	47.0229
53.		116	0	100	43.0444	43.1406	31.9503	42.0291	46.2930	45.0701
54.		81	0	150	95.3791	97.9346	146.8197	128.3143	87.0087	91.1115
55.		64	0	150	134.1229	147.8063	95.3558	142.1814	97.1495	99.4261
56.		117	0	40	15.9465	16.0712	17.8543	19.7354	19.5185	20.5103
57.	Voltage (p.u.)	1	0.95	1.1	1.0263	1.0285	1.0389	1.0471	1.0250	1.0111
58.		4	0.95	1.1	1.0310	1.0321	1.0014	1.0050	1.0286	1.0148
59.		6	0.95	1.1	1.0355	1.0349	1.0346	1.0291	1.0207	1.0179
60.		8	0.95	1.1	1.0093	1.0057	1.0157	1.0193	1.0126	1.0203
61.		10	0.95	1.1	1.0374	1.0377	1.0172	1.0024	1.0057	1.0107
62.		12	0.95	1.1	1.0158	1.0146	1.0379	1.0224	1.0187	1.0214
63.		15	0.95	1.1	1.0206	1.0213	1.0179	1.0179	1.0016	1.0111
64.		18	0.95	1.1	1.0285	1.0294	1.0222	1.0259	1.0172	1.0135
65.		19	0.95	1.1	1.0193	1.0191	1.0255	1.0269	1.0224	1.0180

66.		24	0.95	1.1	1.0230	1.0226	1.0228	1.0235	1.0154	1.0256
67.		25	0.95	1.1	1.0278	1.0279	1.0227	0.9998	1.0166	1.0223
68.		26	0.95	1.1	1.0157	1.0143	1.0175	1.0212	1.0346	1.0258
69.		27	0.95	1.1	1.0335	1.0338	1.0151	1.0080	1.0004	1.0126
70.		31	0.95	1.1	1.0378	1.0379	1.0283	1.0260	1.0117	1.0245
71.		32	0.95	1.1	1.0211	1.0218	1.0302	1.0335	1.0150	1.0035
72.		34	0.95	1.1	1.0259	1.0243	1.0269	1.0250	0.9999	1.0059
73.		36	0.95	1.1	1.0379	1.0375	1.0300	1.0142	1.0044	1.0051
74.		40	0.95	1.1	1.0346	1.0340	1.0288	1.0075	1.0088	1.0236
75.		42	0.95	1.1	1.0239	1.0232	1.0269	1.0040	1.0034	1.0187
76.		46	0.95	1.1	1.0123	1.0124	1.0189	1.0215	1.0216	1.0224
77.		49	0.95	1.1	1.0274	1.0285	1.0157	0.9947	1.0179	1.0163
78.		54	0.95	1.1	1.0252	1.0259	1.0211	1.0138	1.0034	1.0197
79.		55	0.95	1.1	1.0079	1.0078	1.0370	1.0267	1.0203	1.0203
80.		56	0.95	1.1	1.0059	1.0040	1.0313	1.0278	1.0147	1.0172
81.		59	0.95	1.1	1.0022	1.0021	1.0328	1.0261	1.0193	1.0278
82.		61	0.95	1.1	1.0346	1.0342	1.0202	1.0459	1.0223	1.0327
83.		62	0.95	1.1	1.0200	1.0201	1.0132	1.0243	1.0121	1.0174
84.		65	0.95	1.1	1.0282	1.0288	1.0433	1.0170	1.0304	1.0022
85.		66	0.95	1.1	1.0376	1.0301	1.0247	1.0277	0.9996	1.0391
86.		69	0.95	1.1	1.0270	1.0266	1.0247	1.0202	1.0051	0.9985
87.		70	0.95	1.1	1.0283	1.0231	1.0293	1.0337	1.0106	1.0107
88.		72	0.95	1.1	1.0330	1.0334	1.0173	1.0119	1.0223	1.0256
89.		73	0.95	1.1	1.0417	1.0415	1.0185	1.0283	1.0146	1.0270
90.		74	0.95	1.1	1.0268	1.0314	0.9992	1.0272	1.0090	1.0156
91.		76	0.95	1.1	1.0088	1.0051	1.0253	1.0119	1.0085	1.0071
92.		77	0.95	1.1	1.0187	1.0192	1.0427	1.0314	1.0021	1.0065
93.		80	0.95	1.1	1.0252	1.0254	1.0217	1.0404	1.0176	1.0109
94.		85	0.95	1.1	1.0134	1.0140	1.0065	1.0240	1.0061	1.0142
95.		87	0.95	1.1	1.0207	1.0182	1.0373	1.0161	1.0299	1.0236
96.		89	0.95	1.1	1.0214	1.0210	1.0293	1.0363	1.0298	1.0384
97.		90	0.95	1.1	1.0218	1.0209	1.0132	1.0280	1.0272	1.0248
98.		91	0.95	1.1	1.0264	1.0243	1.0225	1.0480	1.0097	1.0340
99.		92	0.95	1.1	1.0262	1.0276	1.0243	1.0312	1.0201	1.0213
100.		99	0.95	1.1	1.0083	1.0065	1.0235	1.0415	1.0471	1.0092
101.		100	0.95	1.1	1.0155	1.0091	1.0263	1.0291	1.0145	1.0414
102.		103	0.95	1.1	1.0270	1.0280	1.0238	1.0226	1.0348	1.0165
103.		104	0.95	1.1	1.0178	1.0168	1.0251	1.0103	1.0264	1.0018
104.		105	0.95	1.1	1.0316	1.0352	1.0296	1.0118	1.0302	1.0263
105.		107	0.95	1.1	1.0132	1.0127	1.0197	1.0042	1.0110	1.0340
106.		110	0.95	1.1	1.0212	1.0226	1.0144	1.0117	1.0140	1.0164
107.		111	0.95	1.1	1.0209	1.0203	1.0166	0.9956	1.0218	1.0386
108.		112	0.95	1.1	1.0184	1.0181	1.0249	1.0163	1.0233	1.0227
109.		113	0.95	1.1	1.0333	1.0331	1.0292	1.0343	1.0289	1.0223
110.		116	0.95	1.1	1.0418	1.0409	1.0044	1.0108	1.0042	1.0088
111.	Tap ratio	8	0.9	1.1	1.0165	1.0157	1.0369	0.9994	1.0045	0.9733
112.		32	0.9	1.1	1.0025	1.0020	0.9801	0.9958	0.9807	1.0123
113.		36	0.9	1.1	0.9948	0.9871	1.0081	0.9237	0.9941	0.9875
114.		51	0.9	1.1	1.0136	1.0109	1.0080	0.9826	0.9739	0.9739
115.		93	0.9	1.1	0.9876	0.9848	0.9975	0.9304	0.9834	0.9874
116		95	0.9	1.1	0.9931	0.9944	0.9947	0.9980	1.0004	0.9681
117.		102	0.9	1.1	1.0057	1.0068	0.9798	0.9999	0.9913	1.0148
118.		107	0.9	1.1	0.9818	0.9817	0.9925	0.9784	0.9780	0.9813
119.		127	0.9	1.1	0.9806	0.9842	0.9931	0.9861	1.0129	1.0087
120.	Shunt VAR compensator (MVAR)	34	0	25	11.3179	11.3041	11.8443	14.5351	15.6509	11.2427
121.		44	0	25	10.0859	10.2002	13.0331	14.2184	10.0191	8.9692
122.		45	0	25	14.7235	14.7171	12.0710	9.0981	10.7855	14.2602
123.		46	0	25	13.0587	13.5962	12.6628	6.1809	9.0046	8.7527
124.		48	0	25	11.7728	11.7501	12.2913	14.5904	10.2403	12.7883
125.		74	0	25	12.4274	12.8144	13.8217	14.0292	11.4761	12.4056
126.		79	0	25	12.0556	11.9471	10.6996	6.2538	11.0239	15.1773
127.		82	0	25	16.3087	16.5841	13.5684	16.4578	12.8005	12.9986
128.		83	0	25	11.7913	11.7448	8.8350	11.4913	9.8887	14.9399
129.		105	0	25	12.6136	12.5949	12.5140	10.6581	12.8361	14.2250
130.		107	0	25	8.8002	9.3753	15.4349	12.8524	10.2346	11.5393
131.		110	0	25	11.7193	11.8521	16.3327	15.2300	12.9425	12.0121
1.	TC($/h)	-	-	-	129019.12	129582.23	130673.5	130796.33	134395.5	133574.6
2.	APL(MW)	-	-	-	36.7616	37.3464	38.0368	32.5358	40.0724	41.3020
3.	VMD (p.u)	-	-	-	-	-	-	0.5165	0.6876	0.9706

5.3.2. Case-12: Minimize TC, APL and VMD simultaneously

In this case, TC, APL, and VMD are the objectives that need to be minimized simultaneously. The optimal decision variables obtained by the suggested method are included in Table 8. The best-compromised values using the proposed algorithm have a total cost of 130796.33$/h, APL of 32.5358MW, and VMD of 0.5165p.u., which is the lowest value compared with NSGA-II [40] and MOPSO [41] as reported in Table 8. The best compromised values achieved using the above methods are 134395.5$/h, 40.0724MW, 0.6876p.u. and 133574.6$/h, 41.3020MW, 0.9706p.u.respectively. Fig.11 depicts the PO fronts for each approach.

5.4. Statistical Analysis

The statistical inference including best value, worst value, and percentage of errors for Case-6 and Case-11 of IEEE 57 and 118-bus power systems are tabulated in Tables 9a-9b. From Tables 9a-9b, it is evident that the proposed algorithm shows better performance compared to NSGA-II and MOPSO methods.

Table 9a. IEEE 57-bus system: Statistical inferences for Case-6

Algorithms	Objectives	Case-6		
		Best value	Worst value	% Error
Proposed Method	TC($/h)	3.557E+4	3.645E+4	2.42
	TE(ton/h)	0.833	0.9545	12.72
NSGA-II [40]	TC($/h)	3.536E+4	3.742E+4	5.49
	TE(ton/h)	0.8097	1.138	28.81
MOPSO [41]	TC($/h)	3.534E+4	3.686E+4	4.10
	TE(ton/h)	0.9391	1.203	21.91

Table 9b. IEEE 118-bus system: Statistical inferences for Case-11

Algorithms	Objectives	Case-11		
		Best value	Worst value	% Error
Proposed Method	TC($/h)	1.283E+5	1.296E+5	0.95
	APL(MW)	36.38	39.19	7.17
NSGA-II [40]	TC($/h)	1.291E+5	1.309E+5	1.37
	APL(MW)	35.04	40.38	13.22
MOPSO [41]	TC($/h)	1.302E+5	1.333E+5	2.36
	APL(MW)	36.09	45.04	19.87

Table 10a. Case-1: TC ($/h)

Variation	SS	df	MS	F	P-value
Between-group	326734	2	163367	140.37	1.2215E-43
Within-group	345656.4	297	1163.8	-	-
Total	672390.4	299	-	-	-

Table 10b. Case-1: TE (ton/h)

Variation	SS	df	MS	F	P-value
Between-group	0.00515	2	0.00257	29.81	1.5912E-12
Within-group	0.02564	297	0.00009	-	-
Total	0.03079	299	-	-	-

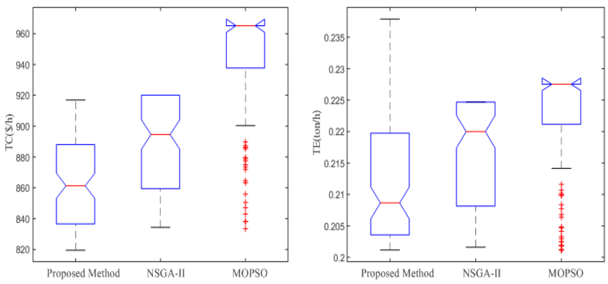

Fig.12(a) Fig.12(b)

Fig.12. Case-1: IEEE 30-bus system: Box plots of best-compromised values

To further instigate the efficiency and robustness of the proposed algorithm on the MOOPF problem, one-way analysis of variance (ANOVA) [8] test was conducted to analyze the statistical significance of each of the tested algorithms over other algorithms. ANOVA is a statistical test that is used to determine the mean of many strategies generated for each trial that exhibits a significant difference. Within-group variation quantifies the degree to which individuals deviate from the group mean. The term "residual" refers to the difference between an individual's value and the group mean. The squares of these residuals are joined together to obtain the sum of squares (SS_{within}). Between-group variation quantifies the degree to which group means deviate from the mean for the entire population ($SS_{between}$). This is done by conducting a hypothesis test to ensure the techniques' robustness. Here, the degree of significance is set to 0.05 to account for the variability in all of the procedures used in the hypothesis test. The F-ratio is calculated as the ratio of two mean square (MS) values. The P-values are calculated using the F-ratio, and the two degrees of freedom (df) are listed in Tables10a-10b. If the P-value for the one-way ANOVA test is less than 0.05, there is adequate evidence that one or more approaches are statistically different from one another.

The statistical studies were also performed using box plots. A box plot is a graphical tool that summarizes numerous critical parameters in a distribution visually. A box plot ranges from the lower hinge (25th percentile) to the top hinge (75th percentile) and contains the distribution's middle half of scores. The median is denoted by a line that passes through the centre of the box. Thus, one-fourth of the distribution resides between this line and the box's top, and one-fourth lies between this line and the box's bottom. The box plots for the best-compromised values of Case-1 are shown in Fig.12. It shows that the proposed method achieves the best variance of distribution and mean value over other algorithms, which means that the proposed algorithm is more robust than other algorithms. From box plots, it is clear that the proposed algorithm gives better results. From all the ANOVA results, it is concluded that the proposed algorithm gives the best optimal results over other algorithms on the MOOPF problem.

6. CONCLUSIONS

This paper presents a solution to the MOOPF problem by combining Wind, PV, and PEV systems. The approach is based on MOEA-based decomposition and summing up of normalized objective functions with an improved diverse selection mechanism. It also deals with tackling various constraints in the MOOPF problem using the superiority of the feasible solution (SF) technique. The cost of thermal energy and the cost uncertainty associated with Wind, PV, and PEV energy systems are minimized along with the minimization of carbon emission, active power losses, and voltage magnitude deviation. Monte-Carlo simulations were used to assess the uncertainty of Wind, PV, and PEV power. Apart from conventional cost minimization, this paper chose factors that account for uncertain prices of available Wind, PV, and PEV power. It showed the OPF formulation along with factors affecting Wind, PV, and PEV power's intermittency. To show the efficacy of the proposed method, simulations were done on the same test systems as with NSGA-II and MOPSO algorithms. The results show the superiority of the suggested method compared to other methods. The statistical analysis using the ANOVA test validates the proposed method by demonstrating that its mean is significantly superior from NSGA-II and MOPSO approaches. Further research can consider innovative OPF problems, such as varying time instances to model real-time changes in load demand including RESs and PEVs. The limitations of the proposed method are that the performance of this method depends on parameter settings and computing time grows as the number of objectives increases. Hence, the suggested method can be effectively used in operation when Wind, PV, and PEV power generations are included in the power system.

REFERENCES

[1] P. Biswas et al., "Multi-objective economic-environmental power dispatch with stochastic wind-solar-small hydro power", *Energy*, vol.150, pp.1039-1057, 2018.

[2] D. Molzahm, "Identifying and characterizing non-convexities in feasible spaces of optimal power flow problems", *IEEE Trans. Circuits Syst. II.*, vol. 65(5), pp. 672-676, 2018.

[3] D. Wu et al., "A deterministic method to identify multiple local extreme for the AC optimal power flow problem", *IEEE Trans. Power Syst.*, vol. 33(1), pp. 654-668, 2018.

[4] H. Dommel, W. Tinney, "Optimal power flow solutions", *IEEE Trans. Power Appar. Syst.*, vol.87, pp.1866-1876, 1968.

[5] M. Lin et al., "A hybrid current-power optimal power flow technique", *IEEE Trans. Power Syst.*, vol. 23(1), pp.177-185, 2008.

[6] W. Yan et al., "A new optimal reactive power flow model in rectangular form and its solution by predictor corrector primal dual interior point method", *IEEE Trans. Power Syst.*, vol. 21(1), pp.61-67, 2006.

[7] S. Duman et al., "Symbiotic organisms search algorithm-based security-constrained AC-DC OPF regarding uncertainty of wind, PV and PEV systems", *Soft Comput.*, vol. 25, pp. 9389-9426, 2021.

[8] J. Sarda et al., "Dynamic optimal power flow with cross entropy covariance matrix adaption evolutionary strategy for systems with electric vehicles and renewable generators", *Int J Energy Res.*, pp. 1-13, 2021.

[9] S. Duman, J. Li, L. Wu, "AC optimal power flow with thermal-wind-solar-tidal systems using the symbiotic organisms search algorithm", *IET Renew. Power Gener.*, vol. 15, pp. 278-296, 2021.

[10] H. Ben, T. Chambers and J. Lee, "Solving constrained optimal power flow with renewables using hybrid modified imperialist competitive algorithm and sequential quadratic programming", *Elect. Power Syst. Research.*, vol.177, p.105989, 2019.

[11] A. Thorat, I. Korachgaon and A. Mulla, "Optimization of fuel cost incorporating with wind, solar PV and Electric vehicle energy sources using improved artificial bee colony algorithm", *Int. J. Electr. Engg. Tech. (IJEET)*, vol. 12(6), pp. 19-18, 2021.

[12] K. Nusair and F. Alasali, "Optimal power flow management system for a power network with stochastic

renewable energy resources using golden ratio optimization method", *Energies*. vol.13, 2020.
[13] M. Sulaiman and Z. Mustaffa, "Solving optimal power flow problem with stochastic wind-solar-small hydro power using barnacles mating optimizer", *Control Eng. Practice.*, vol. 106, 2021.
[14] S. Pandya and H. Jariwala, "Single and Multi-objective Optimal Power Flow with Stochastic Wind and Solar power Plants Using Moth Flame Optimization Algorithm", *Smart Sci.*, 2021.
[15] H. Bouchekara, "Solution of the optimal power flow problem considering security constraint using an improved chaotic electromagnetic field optimization algorithm", *Neural Comput. Appl.* vol. 32, pp. 2683-2703, 2020.
[16] P. Biswas et al., "Optimal power flow solutions using differential evolution algorithm integrated with effective constraint handling techniques", *Eng. Appl. Artificial Intell.*, vol. 68, pp. 81-100, 2018.
[17] F. Alasali et al., "An analysis of optimal power flow strategies for a power network incorporating stochastic renewable energy resources", *Int. Trans. Electr. Energ. Syst*., 2021.
[18] A. Bhattacharya and P. Roy, "Solution of multi-objective optimal power flow using gravitational search algorithm". *IET Gener. Transm. Distrib*., vol. 6, pp. 751-763, 2012.
[19] A. Jasemi and H. Abdi, "Probabilistic Multi-Objective Optimal Power Flow in an AC/DC hybrid microgird considering emission cost, J. Oper. Autom. Power Eng., vol. 10, pp. 13-27, 2022.
[20] M. Dehghani et al., "FOA: following' optimization algorithm for solving power engineering optimization problems", *J. Oper. Autom. Power Eng.*, vol. 8 (1), pp. 57-64, 2020.
[21] S. Li, W. Gong, L. Wang and Q. Gu. "Multi-objective optimal power flow with stochastic wind and solar power". *Appl. Soft Comput*. vol.114, 2022.
[22] S. Reddy, "Optimal power flow using multi-objective glowworm swarm optimization algorithm in a wind energy integrated power system", *Int. Journal of Green Energy*, vol.16, pp.1547-1561, 2019.
[23] R. Effatnejad et al., "Solving multi-objective optimal power flow using modified GA and PSO based on hybrid algorithm", *J. Oper. Autom. Power Eng.*, vol. 5(1), pp.51-60, 2017.
[24] M. Morshed, J. Hmida and A. Fekih, "A probabilistic multi-objective approach for optimal power flow optimization in hybrid wind-PV-PEV systems". *Appl. Energy*, vol.211, pp. 1136-1149, 2018.
[25] S. Galvani et al., "A multi-objective probabilistic approach for smart voltage control in wind-energy integrated networks considering correlated parameters", *Sustain. Cities Soc.*, vol.78, p.103651, 2022.
[26] S. Sandya, P. Jangir and I. Trivedi, "Multi-objective Moth Flame Optimizer: A Fundamental visions for wind power integrated optimal power flow with FACTS devices", *Smart Sci.*, 2021.
[27] G. Alvarez, "Stochastic optimization considering the uncertainties in the electricity demand, natural gas infrastructures, photovoltaic units, and wind generation", *Comput. Chem. Eng.*, vol.160, p.107712, 2022.
[28] H. Bakhtiari et al., " Predicting the stochastic behavior of uncertainty sources in planning a stand-alone renewable energy-based micro grid using Metropolis-coupled Markov chain Monte Carlo simulation", *Appl. Energy*, vol. 290, p.116719, 2021.
[29] K. Li et al., "An evolutionary many-objective optimization algorithm based on dominance and decomposition", *IEEE Trans. Evol. Comput*, vol. 19(5), pp. 694-716, 2015.
[30] C. Mishra et al., "Optimal power flow in the presence of wind power using modified cuckoo search", *IET Gener. Transm. Distrb*, vol. 9(7), pp.615-626, 2015.
[31] P. Biswas et al., "Optimal power flow solutions incorporating stochastic wind and solar power", *Energy Convers. Manage*, vol.148, pp.1194-1207, 2017.
[32] M. Sulaiman et al., "Optimal power flow with stochastic solar power using barnacles mating optimizer", *Int. Trans. Electr. Energy Syst*., vol. 66, pp. 88-93, 2021.
[33] J. Zhao et al., "Optimal dispatch of electric vehicles and wind power using enhanced particle swarm optimization", *IEEE Trans. Indus. Inform*., vol. 8(4), pp. 889-899, 2012.
[34] P. Hanemann et al., "Effects of electric vehicle charging strategies on the German power system", *Appl. Energy*. vol. 203, pp.608-622, 2017.
[35] T. Wu et al., "Coordinated energy dispatching in micro grid with wind power generation and plug-in electric vehicles". *IEEE Trans. Smart Grid*. vol.4, pp.1453-63, 2013.
[36] K. Deb. "An efficient constraint handling method for genetic algorithms", *Comput. Methods Appl. Mech. Engrg*., vol.186, pp.311-338, 2000.
[37] K. Li et al., "An evolutionary many-objective optimization algorithm based on dominance and decomposition". *IEEE Trans. Evol. Comput*., vol. 19(5), pp.694-716, 2015.
[38] Q. Zhang and H. Li, "MOEA/D: A multi objective evolutionary algorithm based on decomposition", *IEEE Trans. Evol. Comput.*, vol.11(6), pp.712-731, 2007.
[39] B. Qu and P. Suganthan, "Multi-objective differential evolution based on the summation of normalized objectives and improved selection method", *IEEE Symp.*, pp.1-8, 2011.
[40] K. Deb et al., "A fast and elitist multi objective genetic algorithm: NSGA-II", *IEEE Trans. Evol. Comput.*, vol.6(2), pp.182-197, 2002.
[41] C. Coello, G. Pulido, and M. Lechuga. "Handling multiple objectives with particle swarm optimization", *IEEE Trans. Evol. Comput*., vol. 8(3), pp.256-279, 2004.
[42] I. Das and J. Dennis. "Normal–boundary intersection: A new method for generating Pareto optimal points in multi-criteria optimization problems", *SIAM J. Optimiz.*, vol. 8(3), pp.631-657, 1998.
[43] Y. Zhang and Y. Li. "A many-objective evolutionary algorithm based on decomposition and local dominance", 2018.
[44] B. Qu and P. Suganthan, "Multi-objective evolutionary algorithms based on the summation of normalized objectives and diversified selection", *Inf. Sci.*, vol.180 (17), pp.3170-3181, 2010.
[45] R. Zimmerman et al., "MATPOWER: Steady-state operations, planning, and analysis tools for power systems research and education", *IEEE Trans. Power Syst*., vol. 26, pp. 9-12, 2011.